Koopmans-like Approximation in the Kohn−Sham Method and the Impact of the Frozen Core Approximation on the Computation of the Reactivity Parameters of the Density Functional Theory

Rubicelia Vargas,* Jorge Garza, and Andrés Cedillo

Departamento de Química, Universidad Autónoma Metropolitana Iztapalapa, Apartado Postal 55-534, San Rafael Atlixco 186, Col. Vicentina. Del. Iztapalapa. C.P. 09340. México, D.F. México

Received: April 22, 2005; In Final Form: July 29, 2005

A Koopmans-like approximation is introduced in the spin-polarized version of the Kohn−Sham (KS) density functional theory to obtain a relation between KS orbital energies and vertical ionization potential and electron affinity. Expressions for reactivity indexes (like electronegativity, hardness, electrophilicity, and excitation energies) include KS frontier orbital energies and additional contributions associated with the self-interaction correction. Those reactivity parameters were computed with different exchange-correlation functionals to test the approach for a set of small molecules. The results show that the present approximation provides a better way to estimate hardness, electronegativity, and electrophilicity than just the use of frontier orbital energy values. However KS HOMO and LUMO energy gap gives a better agreement with excitation energies.

I. Introduction

At this time there are two well-established theories to aboard the study of the electronic structure of a chemical system. The traditional quantum chemistry based on the Schrödinger equation solution and the density functional theory (DFT) where the electron density is the main variable.[1] DFT has been successfully applied to predict many properties of ground state with high accuracy and with less computational effort than some of the traditional ab initio methods. This important feature has made DFT a more frequently used methodology in many different problems in a successfully way, mainly in large systems.[2] Besides, this theory has given a framework to rationalize some empirical concepts such as electronegativity,[3] hardness,[4] and softness[5] and has provided some new ones such as spin potential,[6] electrophilicity,[7] and Fukui functions.[8] The study of these reactivity parameters in DFT is an active field, which is widely used to get a better understanding of the chemical reactivity of atoms, molecules, clusters, and solids.

DFT was born in 1964 when Hohenberg and Kohn established their two theorems.[9] But in 1965, Kohn and Sham (KS)[10] provided the most powerful approach to use this theory in a practical way. The main contribution of their proposal was the introduction of orbitals to compute exactly one part of the kinetic energy. A detailed explanation of the KS approach can be found in the literature;[1] however, we want to emphasize that the introduction of the KS orbitals was really relevant in the development of DFT. These KS orbitals were originally introduced only as a practical tool, and no physical meaning was initially attributed to them. Despite this, many authors have extended the meaning of the Hartree−Fock (HF) orbital energies to the KS case, and one can found that in many cases the Koopmans' theorem[11] is used in the same way in both theories.[12] For example, to evaluate the hardness of a chemical system, the difference between the HOMO and LUMO energies has been indistinctly used with both KS and HF orbitals.[12,13] But, does the KS orbitals have the same physical meaning that the chemists look for? Could we relate the orbital energies emerged from a KS calculation with the ionization potential, the electron affinity, or other properties?

Some authors opened this discussion in the literature.[14] It has been proved that the KS orbitals must be carefully used when we want to rationalize chemical phenomena with them; symmetry, ordering, and shape of orbitals must be checked.[15] There are two important results related with the exchange-correlation potentials that contain the correct asymptotic behavior: (1) A relationship between the HOMO KS eigenvalue and the ionization potential has been established.[16] Although this relationship has been criticized,[17] there is strong evidence that it is valid when an exchange-correlation potential with the appropriate asymptotic behavior is used.[15,18,19] (2) It has been found a good agreement between the KS HOMO−LUMO difference and the lowest excitation energy.[20] This agreement is explained by the similarity of the equations from many-body quasiparticle and KS theories.[21] However, these two important results are not satisfied by many of the exchange-correlation functionals commonly used, mainly because these functionals do not cancel properly the self-interaction energy; consequently, the corresponding exchange-correlation potentials show an incorrect asymptotic behavior.[22]

It is well-known that many of the frequently used exchange-correlation functionals do not correctly cancel the Coulomb contribution of each electron with the corresponding exchange part, this spurious remainder is known as the self-interaction energy.[1,23] If this self-interaction contribution is not appropriately canceled, some chemical events cannot be adequately described. In this paper we show that the self-interaction plays an important role on the computation of electronic properties such as ionization potential, electronegativity, hardness, electrophilicity, and singlet−triplet excitation energy. To estimate these quantities we approximate the vertical energy differences within the frozen core approximation using the spin-polarized version of the KS DFT. The resulting expressions for removal or addition of one electron to an electronic system can be evaluated after

* Corresponding author e-mail: ruvf@xanum.uam.mx.

10.1021/jp052111w CCC: $30.25
Published on Web 09/14/2005

the self-consistent process. The frozen core approximation means that the relaxation in the geometry and in the orbitals is not considered when the number of electrons is changed in a particular process. Although this approximation suggests a name as frozen orbitals instead of frozen core approximation, we will use the last one since it has been frequently used in the DFT community.[8b]

In section II, a Koopmans-like approximation is introduced in the KS formalism. Processes where the number of electrons changes are treated in section III, and those where the multiplicity is changing are discussed in section IV. Computational details are in section V. Results and discussion related with ionization potential, electron affinity, electronegativity, hardness, electrophilicity, and singlet−triplet excitation energy are presented in section VI. Concluding remarks are given in section VII.

II. Koopmans-like Approximation in the KS Method

The spin-polarized KS energy for a system with N electrons and in the absence of a magnetic field is written as

$$E_{KS}(N) = E_{KS}(N_\alpha, N_\beta) = \sum_{i=1}^{N_\alpha}\left\langle \psi_{\alpha,i}\left| -\frac{1}{2}\nabla^2 \right|\psi_{\alpha,i}\right\rangle + \sum_{i=1}^{N_\beta}\left\langle \psi_{\beta,i}\left| -\frac{1}{2}\nabla^2 \right|\psi_{\beta,i}\right\rangle + \frac{1}{2}\int\int d\mathbf{r}\, d\mathbf{r}'\frac{\rho(\mathbf{r})\rho(\mathbf{r}')}{|\mathbf{r}-\mathbf{r}'|} + E_{XC}[\rho_\alpha, \rho_\beta] + \int d\mathbf{r}\rho(\mathbf{r})v(\mathbf{r}) \quad (1)$$

N_α and N_β represent the number of electrons with spin α and β, respectively, such that $N = N_\alpha + N_\beta$. $E_{XC}[\rho_\alpha, \rho_\beta]$ is the exchange-correlation energy, and $v(\mathbf{r})$ is the external potential, which in free molecules is only due to the nuclei.

The components of the total density are built from the KS spin−orbitals, $\psi_{\sigma,i}$, as

$$\rho(\mathbf{r}) = \sum_{\sigma=\alpha,\beta}\rho_\sigma(\mathbf{r}) = \sum_{\sigma=\alpha,\beta}\sum_{i=1}^{N_\sigma}\rho_{\sigma,i}(\mathbf{r}) = \sum_{\sigma=\alpha,\beta}\sum_{i=1}^{N_\sigma}\psi^*_{\sigma,i}(\mathbf{r})\psi_{\sigma,i}(\mathbf{r}) \quad (2)$$

where $\rho_{\sigma,i}$ is a spin−orbital density and ρ_σ is the electron density associated with spin σ.

The KS spin−orbitals are those that minimize the total energy; therefore, they satisfy the integro-differential KS equations:

$$\left\{\hat{h}(\mathbf{r}) + \int d\mathbf{r}'\frac{\rho(\mathbf{r}')}{|\mathbf{r}-\mathbf{r}'|} + \frac{\delta E_{XC}[\rho_\alpha, \rho_\beta]}{\delta\rho_\sigma(\mathbf{r})}\right\}\psi_{\sigma,i} = \epsilon_{\sigma,i}\psi_{\sigma,i} \quad (3)$$

where the operator $\hat{h}$ is defined as

$$\hat{h}(\mathbf{r}) = -\frac{1}{2}\nabla^2 + v(\mathbf{r}) \quad (4)$$

and $v_{XC,\sigma}(\mathbf{r}) \equiv \delta E_{XC}/\delta\rho_\sigma(\mathbf{r})$ is the exchange-correlation potential for spin σ, which corresponds to a first functional derivative of the exchange-correlation energy functional. From eq 3, the KS orbital energy takes the following form:

$$\epsilon_{\sigma,i} = \langle\psi_{\sigma,i}|\hat{h}|\psi_{\sigma,i}\rangle + \left\langle \psi_{\sigma,i}\left| \int d\mathbf{r}'\frac{\rho(\mathbf{r}')}{|\mathbf{r}-\mathbf{r}'|} + v_{XC,\sigma}(\mathbf{r})\right|\psi_{\sigma,i}\right\rangle \quad (5)$$

In the frozen core approximation the electronic state P is approximately described by the orbitals of a related reference state Q, using Koopmans' ideas. For the reference state Q, the KS energy is given by eq 1:

$$\begin{aligned} E^Q_{KS} &\equiv E_{KS}(N^Q_\alpha, N^Q_\beta) = E_{KS}[|D^Q_{KS}\rangle] = E_{KS}[|\phi^Q_1\,\phi^Q_2\cdots\phi^Q_{N_Q}|] \\ &= \sum_{i=1}^{N_Q}\left\langle \phi^Q_i\left| -\frac{1}{2}\nabla^2\right|\phi^Q_i\right\rangle + \int d\mathbf{r}\rho^Q(\mathbf{r})v(\mathbf{r}) + \frac{1}{2}\int\int d\mathbf{r}\, d\mathbf{r}'\frac{\rho^Q(\mathbf{r})\rho^Q(\mathbf{r}')}{|\mathbf{r}-\mathbf{r}'|} + E_{XC}[\rho^Q_\alpha, \rho^Q_\beta] \\ &= T_S[\phi^Q_1, \phi^Q_2, \cdots \phi^Q_{N_Q}] + \int d\mathbf{r}\rho^Q(\mathbf{r})v(\mathbf{r}) + J[\rho^Q] + E_{XC}[\rho^Q_\alpha, \rho^Q_\beta] \\ &= T^Q_S + \int d\mathbf{r}\rho^Q(\mathbf{r})v(\mathbf{r}) + J^Q + E^Q_{XC} \end{aligned} \quad (6)$$

where the KS spin−orbitals were renumbered for a short notation, $|D^Q_{KS}\rangle$ is the KS determinant for this state, T_S represents the noninteracting kinetic energy functional, J corresponds to the classical Coulombic repulsion energy, and the electron density for this state comes from eq 2, namely

$$\rho^Q(\mathbf{r}) = \rho^Q_\alpha(\mathbf{r}) + \rho^Q_\beta(\mathbf{r}) = \sum_{i=1}^{N_Q}|\phi^Q_i(\mathbf{r})|^2 \quad (7)$$

Since the KS orbitals for the state Q satisfy eq 5, then the corresponding energy can be written in the form

$$E^Q_{KS} = \sum_{i=1}^{N_Q}\epsilon^Q_i - J^Q + E^Q_{XC} - \sum_{\sigma=\alpha,\beta}\int d\mathbf{r}\rho^Q_\sigma(\mathbf{r})v^Q_{XC,\sigma}(\mathbf{r}) \quad (8)$$

and

$$v^Q_{XC,\sigma}(\mathbf{r}) \equiv v_{XC,\sigma}(\mathbf{r})|_{\rho_\alpha{}^Q,\rho_\beta{}^Q} \equiv \left.\frac{\delta E_{XC}}{\delta\rho_\sigma(\mathbf{r})}\right|_{\rho_\alpha{}^Q,\rho_\beta{}^Q} \quad (9)$$

The properties of the state P must be obtained from the KS determinant associated to this state, $|D^P_{KS}\rangle$. In the frozen core approximation, the properties of the state P come from a KS determinant constructed with the reference state orbitals, $|D^{P(Q)}_{KS}\rangle$, that is,

$$|D^P_{KS}\rangle \equiv |\phi^P_1\,\phi^P_2\cdots\phi^P_{NP}| \approx |D^{P(Q)}_{KS}\rangle \equiv |f^P_1\,f^P_2\cdots f^P_{NP}| \quad (10)$$

where the orbitals $\{f^P_i\}$ correspond to a subset of the KS orbitals from state Q

$$f^P_i = \phi^Q_{a_i}, \quad \begin{pmatrix} i = 1, 2, \cdots, N_P \\ a_i \in \{1, 2, \cdots\}\end{pmatrix} \quad (11)$$

Note that the state P can have a different number of electrons or just a change in its multiplicity. In the former case, unoccupied KS orbitals must be added when the number of electrons increases, or some of them must be removed if the number of electrons decreases. For the latter case, unoccupied orbitals must be added to one spin set, while the same number of occupied orbitals must be removed from the other spin

branch. Thus, the KS energy of the state P can be approximated by

$$\begin{aligned} E_{\mathrm{KS}}^{P} &\equiv E_{\mathrm{KS}}(N_\alpha^P, N_\beta^P) \\ &\approx E_{\mathrm{KS}}^{P(Q)} \equiv E_{\mathrm{KS}}[|D_{\mathrm{KS}}^{P(Q)}\rangle] = E_{\mathrm{KS}}[|f_1^P f_2^P \cdots f_{\mathrm{N_p}}^P|] \\ &= \sum_{i=1}^{N_P}\left\langle f_i^P\right| -\frac{1}{2}\nabla^2\left|f_i^P\right\rangle + \int \mathrm{d}\mathbf{r}\rho^{P(Q)}(\mathbf{r})v(\mathbf{r}) + J[\rho^{P(Q)}] + \\ &\qquad E_{\mathrm{XC}}[\rho_\alpha^{P(Q)}, \rho_\beta^{P(Q)}] \\ &= T_{\mathrm{S}}^{P(Q)} + \int \mathrm{d}\mathbf{r}\rho^{P(Q)}(\mathbf{r})v(\mathbf{r}) + J^{P(Q)} + E_{\mathrm{XC}}^{P(Q)} \end{aligned} \tag{12}$$

where

$$J^{P(Q)} \equiv J[\rho^{P(Q)}],\ E_{\mathrm{XC}}^{P(Q)} \equiv E_{\mathrm{XC}}[\rho_\alpha^{P(Q)}, \rho_\beta^{P(Q)}] \tag{13}$$

$\rho^{P(Q)}$ is the frozen core density of the state P, constructed with orbitals coming from the reference state Q:

$$\rho^{P(Q)} \equiv \sum_{i=1}^{N_P}|f_i^P|^2 = \sum_{i=1}^{N_P}|\phi_{a_i}^Q|^2 \tag{14}$$

and a similar expression for the spin components of the density. Since the orbitals $\{f_i^P\}$ also satisfy eq 5, then

$$\begin{aligned} \sum_{i=1}^{N_P}\epsilon_{a_i}^Q &= T_{\mathrm{S}}^{P(Q)} + \int \mathrm{d}\mathbf{r}\rho^{P(Q)}(\mathbf{r})v(\mathbf{r}) + \\ &\int\int \mathrm{d}\mathbf{r}\,\mathrm{d}\mathbf{r}'\frac{\rho^{P(Q)}(\mathbf{r})\rho^Q(\mathbf{r}')}{|\mathbf{r}-\mathbf{r}'|} + \sum_{\sigma=\alpha,\beta}\int \mathrm{d}\mathbf{r}\rho_\sigma^{P(Q)}(\mathbf{r})v_{\mathrm{XC},\sigma}^Q(\mathbf{r}) \end{aligned} \tag{15}$$

and

$$\begin{aligned} E_{\mathrm{KS}}^{P(Q)} = \sum_{i=1}^{N_P}\epsilon_{a_i}^Q &- \int\int \mathrm{d}\mathbf{r}\,\mathrm{d}\mathbf{r}'\frac{\rho^{P(Q)}(\mathbf{r})\rho^Q(\mathbf{r}')}{|\mathbf{r}-\mathbf{r}'|} + \\ &\frac{1}{2}\int\int \mathrm{d}\mathbf{r}\,\mathrm{d}\mathbf{r}'\frac{\rho^{P(Q)}(\mathbf{r})\rho^{P(Q)}(\mathbf{r}')}{|\mathbf{r}-\mathbf{r}'|} - \\ &\sum_{\sigma=\alpha,\beta}\int \mathrm{d}\mathbf{r}\rho_\sigma^{P(Q)}(\mathbf{r})v_{\mathrm{XC},\sigma}^Q(\mathbf{r}) + E_{\mathrm{XC}}^{P(Q)} \end{aligned} \tag{16}$$

Finally, the estimated vertical energy change takes the form

$$\begin{aligned} E_{\mathrm{KS}}^{P(Q)} - E_{\mathrm{KS}}^{Q} = \sum_{i=1}^{N_P}\epsilon_{a_i}^Q - \sum_{i=1}^{N_Q}\epsilon_i^Q + J[\Delta\rho] + E_{\mathrm{XC}}^{P(Q)} - E_{\mathrm{XC}}^{Q} - \\ \sum_{\sigma=\alpha,\beta}\int \mathrm{d}\mathbf{r}\Delta\rho_\sigma(\mathbf{r})v_{\mathrm{XC},\sigma}^Q(\mathbf{r}) \end{aligned} \tag{17}$$

where $\Delta\rho \equiv \rho^{P(Q)} - \rho^Q$ and $\Delta\rho_\sigma \equiv \rho_\sigma^{P(Q)} - \rho_\sigma^Q$. Note that

$$E_{\mathrm{XC}}^{P(Q)} \equiv E_{\mathrm{XC}}[\rho_\alpha^{P(Q)}, \rho_\beta^{P(Q)}] = E_{\mathrm{XC}}[\rho_\alpha^Q + \Delta\rho_\alpha, \rho_\beta^Q + \Delta\rho_\beta] \tag{18}$$

and a Taylor expansion can be used on the exchange-correlation functional around the reference system; therefore, this expansion leads to

$$\begin{aligned} E_{\mathrm{KS}}^{P(Q)} - E_{\mathrm{KS}}^{Q} = \sum_{i=1}^{N_P}\epsilon_{ai}^Q - \sum_{i=1}^{N_Q}\epsilon_i^Q + \\ \frac{1}{2}\sum_{\sigma,\sigma'=\alpha,\beta}\int\int \mathrm{d}\mathbf{r}\,\mathrm{d}\mathbf{r}'\Delta\rho_\sigma(\mathbf{r})\Delta\rho_{\sigma'}(\mathbf{r}')\left.\frac{\delta^2(J+E_{\mathrm{XC}})}{\delta\rho(\mathbf{r})\delta\rho(\mathbf{r}')}\right|_{\rho_\alpha^Q,\rho_\beta^Q} + \cdots \end{aligned} \tag{19}$$

where the first-order terms vanish. Additional approximations arise if a finite number of terms are kept from the Taylor expansion. It is worth to note that the Coulomb part contributes just to the second order since derivatives of superior order vanish.

In addition, from the variational theorem, $E_{\mathrm{KS}}^{P(Q)} > E_{\mathrm{KS}}^{P}$, then the frozen core vertical energy change always overestimates the true vertical value:

$$\Delta E_{\mathrm{V}} \equiv E_{\mathrm{KS}}^{P} - E_{\mathrm{KS}}^{Q} < E_{\mathrm{KS}}^{P(Q)} - E_{\mathrm{KS}}^{Q} \tag{20}$$

III. Changes in the Number of Electrons

In this section we will discuss quantities that involve changes in the number of electrons such as the ionization potential (IP) and the electron affinity (EA). Within this paper we will work with the frozen core approximation, which means that we will describe all the chemical processes just with information of one state, the reference state Q. So we will suppose that the relaxation of the geometry and spin−orbitals are negligible, and in this sense we are preserving the Koopmans' idea.

Ionization Potential. In this process we only remove one electron, and it can be taken from either the α or β set. If σ' stands for the spin type of the removed electron, then $\Delta N_\sigma = -\delta_{\sigma,\sigma'}$ and $\Delta\rho_\sigma = -\delta_{\sigma,\sigma'}\rho_{\sigma H}$, where $\rho_{\sigma H}$ is the orbital density of the HOMO in the σ spin set and δ_{ij} is the Kronecker's delta symbol. In this case P and $P(Q)$ are states with $N-1$ electrons, while Q contains N electrons. Note that we are subtracting one electron from the HOMO (H) in order to keep the validity of KS theory and to avoid holes in the electronic configuration.

For an open-shell system the removed electron comes from the α component because in such a case $\epsilon_{\alpha,H} > \epsilon_{\beta,H}$, and for a closed-shell system there is no difference in the component where the electron is removed since $\epsilon_{\alpha,H} = \epsilon_{\beta,H}$, then in both cases the orbital $\psi_{\alpha H}$ is involved. Therefore, eq 17 for the IP takes the form

$$\mathrm{IP} = E_{\mathrm{KS}}^{N-1} - E_{\mathrm{KS}}^{N} \approx -\epsilon_{\alpha,H}^N + J[\rho_{\alpha H}] + \int \rho_{\alpha H}v_{\mathrm{XC},\alpha}^{(N)}\,\mathrm{d}\mathbf{r} + \Delta E_{\mathrm{XC}}^{\mathrm{IP}} \tag{21}$$

with

$$\Delta E_{\mathrm{XC}}^{\mathrm{IP}} = E_{\mathrm{XC}}[\rho_\alpha^{(N)} - \rho_{\alpha H}, \rho_\beta^{(N)}] - E_{\mathrm{XC}}[\rho_\alpha^{(N)}, \rho_\beta^{(N)}] \tag{22}$$

Equation 21 shows that the estimation of IP is different than the Koopmans theorem, because in HF method IP is directly identified with the negative of the HOMO energy.[18] In KS method there are three additional terms to the HOMO energy. The contribution from these terms must be small if the exact exchange-correlation potential is used. The main characteristics of the exact exchange-correlation potential are that it must be self-interaction free and it must exhibit the correct asymptotic behavior. Most of the usual exchange-correlation potentials do not satisfy such requirements. We can interpret the additional

terms in eq 21 as a correction to the HOMO energy, coming from the exchange-correlation potentials that do not appropriately cancel the self-interaction contribution, to get a better approximation to the IP.

The strategy is clear, first we have to obtain properties of the reference system Q. Later, we evaluate the terms involved in eq 21, in this way the IP can be estimated just with the information of the reference state. Another procedure to evaluate IP comes from the truncated Taylor expansion given by eq 19. In this particular case it must be evaluated with $\Delta\rho = -\rho_{\alpha H}$:

$$\mathrm{IP} \cong -\epsilon_{\alpha,H} + \frac{1}{2}\int\int \mathrm{d}\mathbf{r}\,\mathrm{d}\mathbf{r}'\left(\frac{\delta^2(J+E_{\mathrm{XC}})}{\delta\rho_\alpha(\mathbf{r})\delta\rho_\alpha(\mathbf{r}')}\right)\rho_{\alpha H}(\mathbf{r})\rho_{\alpha H}(\mathbf{r}') \tag{23}$$

In the exchange-only approach, Gopinathan[24] got a similar equation for the X_α method. However, this author did not take into account the second-order term in the series expansion of the exchange energy; therefore the second derivative of E_{XC} in eq 23 did not appear in his formulation. Thus, there are two ways to approximate the IP. In one case we must evaluate the difference $\Delta E_{\mathrm{XC}}^{\mathrm{IP}}$ and, in the other, this difference is approximated with a series expansion up to second order. In this work we only use the former one for all the cases, since additional approximations to $\Delta E_{\mathrm{XC}}^{\mathrm{IP}}$ are avoided and its computational implementation is easier.

Electron Affinity. In this case an electron is added to the system in the σ' spin set, then $\Delta N_{\sigma'} = \delta_{\sigma,\sigma'}$ and $\Delta\rho_\sigma = \delta_{\sigma,\sigma'}\rho_{\sigma L}$, where $\rho_{\sigma L}$ is the orbital density of the LUMO in the σ spin branch. The reference state Q contains N electrons; P and $P(Q)$ are states with one additional electron. For a closed-shell system the LUMO is equal for both α or β orbitals, but for an open-shell system the electron must be added according to the Hund's high multiplicity rule. Here we restrict our attention to the closed-shell case. The approximation for the electron affinity (EA), given by eq 17, yields

$$\mathrm{EA} = E_{\mathrm{KS}}^{N} - E_{\mathrm{KS}}^{N+1} \approx -\epsilon_{\alpha,L}^{N} - J[\rho_{\alpha L}] + \int \rho_{\alpha L} v_{\mathrm{XC},\alpha}^{(N)}\,\mathrm{d}\mathbf{r} - \Delta E_{\mathrm{XC}}^{\mathrm{EA}} \tag{24}$$

where

$$\Delta E_{\mathrm{XC}}^{\mathrm{EA}} = E_{\mathrm{XC}}[\rho_\alpha^{(N)}, \rho_\beta^{(N)}] - E_{\mathrm{XC}}[\rho_\alpha^{(N)} + \rho_{\alpha L}, \rho_\beta^{(N)}] \tag{25}$$

Although eqs 21 and 24 are similar, the sign for the coulomb integral and the difference between the exchange-correlation energy are different. So it is expected a different behavior between the IP and the EA.

Electronegativity and Hardness. Frequently, the electronegativity and hardness are computed by using the HOMO and LUMO energies. It is well-known that these reactivity indexes are related with derivatives of the total energy; the electronegativity, χ, with the chemical potential, μ, which is the first derivative:[3]

$$\chi = -\mu = -\left(\frac{\partial E}{\partial N}\right)_v \tag{26}$$

and the hardness, η, with the second derivative:[4]

$$\eta = -\left(\frac{\partial^2 E}{\partial N^2}\right)_v \tag{27}$$

It is important to note that both derivatives must be evaluated at the same external potential. Since the external potential is due to the nuclei, the restriction of a fixed external potential means that the geometry in a molecule must be frozen in the process of removing or adding electrons. Using the finite differences approximation, it is obtained that $\chi = (1/2)(\mathrm{IP} + \mathrm{EA})$ and $\eta = (\mathrm{IP} - \mathrm{EA})$. Since the external potential is fixed in the derivatives of eqs 26 and 27, the corresponding IP and EA are related with the corresponding vertical values. In this way both quantities can be approximated in our approach by using eqs 21 and 24. For a closed-shell system the electronegativity is given by

$$\chi \approx -\frac{1}{2}(\epsilon_{\alpha,H} + \epsilon_{\alpha,L}) + (1/2)(J[\rho_{\alpha H}] - J[\rho_{\alpha L}] + \int(\rho_{\alpha H} + \rho_{\alpha L})v_{\mathrm{XC},\alpha}^{(N)}\,\mathrm{d}\mathbf{r} + \Delta E_{\mathrm{XC}}^{\mathrm{IP}} - \Delta E_{\mathrm{XC}}^{\mathrm{EA}}) \tag{28}$$

and the hardness takes the form

$$\eta \approx (\epsilon_{\alpha,L} - \epsilon_{\alpha,H}) + J[\rho_{\alpha H}] + J[\rho_{\alpha L}] + \int(\rho_{\alpha H} - \rho_{\alpha L})v_{\mathrm{XC},\alpha}^{(N)}\,\mathrm{d}\mathbf{r} + \Delta E_{\mathrm{XC}}^{\mathrm{IP}} + \Delta E_{\mathrm{XC}}^{\mathrm{EA}} \tag{29}$$

From here, the electrophilicity can be computed as[7]

$$\omega = \frac{\mu^2}{2\eta} = \frac{\chi^2}{2\eta} \tag{30}$$

The average between the HOMO and LUMO energies is involved in the evaluation of the electronegativity, and the difference between them is required to evaluate the hardness according to eqs 28 and 29. These combinations of the orbital energies are commonly used to estimate electronegativity and hardness, in the context of the KS method; however, there are additional terms that must be taken in account. In this work we explore the contribution of these additional terms and their role in the description of the electronegativity, hardness, and electrophilicity.

IV. Excitation Energies

In section III, we discussed processes where the total number of electrons is changing. However, in processes such as electronic excitation, the number of electrons is constant. In this section we analyze processes involving changes in the multiplicity; consequently, the spin number, $N_{\mathrm{S}} \equiv N_\alpha - N_\beta$, also varies. For example, consider a process where an electron is transferred from the β set to the α one. Note that this process represents an electronic excitation. In this approach we preserve the geometry, so vertical excitation energies or vertical splitting energies are described.

Toward a Higher Multiplicity. In this process the number of electrons from the component α increases, while the number of electrons from the spin β decreases in the same amount to keep N constant. In terms of N_α and N_β, we have

$$\Delta N_\alpha = 1 \quad \Delta N_\beta = -1 \tag{31}$$

This case presents a difference with respect to the processes treated in section III, whereas in those processes N_α or N_β changes, here both N_α and N_β are changing. Since one electron from HOMO β is transferred to the LUMO α, the changes in the spin-densities are

$$\Delta\rho_\alpha = \rho_{\alpha L},\ \Delta\rho_\beta = -\rho_{\beta H} \tag{32}$$

To estimate the energy change involved in this process (HM), we must evaluate eq 17, with $\Delta\rho_\alpha$ and $\Delta\rho_\beta$ from eq 32, to obtain

$$\mathrm{HM} = E_{\mathrm{KS}}^{(N_\alpha+1,N_\beta-1)} - E_{\mathrm{KS}}^{(N_\alpha,N_\beta)} \approx (\epsilon_{\alpha,L} - \epsilon_{\beta,H}) + J[\rho_{\alpha L} - \rho_{\beta H}] + \int(\rho_{\beta H} v_{\mathrm{XC},\beta}^{(N_\alpha,N_\beta)} - \rho_{\alpha L} v_{\mathrm{XC},\alpha}^{(N_\alpha,N_\beta)}) + \Delta E_{\mathrm{XC}}^{\mathrm{HM}} \quad (33)$$

Note that, although in eqs 29 and 33 the difference between the frontier orbital energies appears, these equations are drastically different. First, in eq 33 there is a cross term in the Coulombic contribution that is not present in eq 29. Second, in eq 29, two differences between the exchange-correlation energies are involved, while in eq 33 just one appears, $\Delta E_{\mathrm{XC}}^{\mathrm{HM}} = E_{\mathrm{XC}}[\rho_\alpha + \rho_{\alpha L}, \rho_\beta - \rho_{\beta H}] - E_{\mathrm{XC}}[\rho_\alpha, \rho_\beta]$. Consequently eqs 29 and 33 have different values, and they represent two different quantities, the hardness and an excitation energy, respectively.

Expansion of eq 33 up to second order leads to an expression similar to eq 19:

$$\mathrm{HM} \approx (\epsilon_{\alpha,L} - \epsilon_{\beta,H}) + \frac{1}{2}\int\int \mathrm{d}\mathbf{r}\,\mathrm{d}\mathbf{r}'\frac{\Delta\rho(\mathbf{r}')\Delta\rho(\mathbf{r})}{|\mathbf{r}-\mathbf{r}'|} + \frac{1}{2}\sum_{\sigma,\sigma'=\alpha,\beta}\int\int \mathrm{d}\mathbf{r}\,\mathrm{d}\mathbf{r}'\frac{\delta^2 E_{\mathrm{XC}}}{\delta\rho_\sigma(\mathbf{r})\delta\rho_{\sigma'}(\mathbf{r}')}\Delta\rho_{\sigma'}(\mathbf{r}')\Delta\rho_\sigma(\mathbf{r}) \quad (34)$$

with $\Delta\rho = \Delta\rho_\alpha + \Delta\rho_\beta = \rho_{\alpha H} - \rho_{\beta L}$. Equation 34 constitutes an important result because it relates our approach with the time-dependent DFT approach,[25] if the density current dependence is ignored. To estimate the energy changes when the multiplicity increases, we can use eq 33 or eq 34. We use eq 33 in order to avoid a truncation error from the series expansion. Furthermore, note that the difference between the spin frontier orbital eigenvalues in eqs 33 and 34 represents twice the spin potential (μ_s).[6,26] This reactivity parameter has been defined in the spin-polarized DFT, and it has been used previously with a different approach to estimate vertical singlet−triplet energy gaps in halocarbenes,[27] transition metal ions,[26] free radical generators,[28] and other compounds. Additionally, previous works have directly related the HOMO−LUMO eigenvalue gap with the excitation energy when the exact exchange-correlation potential is used.[19,20] We have found that the excitation energy estimate has additional terms to the HOMO−LUMO difference. Since the exchange-correlation functionals currently used do not have the correct asymptotic behavior and are not self-interaction free, all terms in eq 33 must be kept.

Toward a Lower Multiplicity. The energy change for the decrement in the multiplicity is straightforward using the arguments used in the previous section. In this case we have the following changes:

$$\Delta N_\alpha = -1,\ \Delta N_\beta = 1 \quad (35)$$

and

$$\Delta\rho_\alpha = -\rho_{\alpha H},\ \Delta\rho_\beta = \rho_{\beta L} \quad (36)$$

where we assumed that one electron is transferred from HOMO α to LUMO β. For this case the energy change (LM) is

$$\mathrm{LM} = E_{\mathrm{KS}}^{(N_\alpha-1,N_\beta+1)} - E_{\mathrm{KS}}^{(N_\alpha,N_\beta)} \approx (\epsilon_{\beta,L} - \epsilon_{\alpha,H}) + J[\rho_{\beta L} - \rho_{\alpha H}] + \int(\rho_{\alpha H} v_{\mathrm{XC},\alpha}^{(N_\alpha-N_\beta)} - \rho_{\beta L} v_{\mathrm{XC},\beta}^{(N_\alpha-N_\beta)})\,\mathrm{d}\mathbf{r} + \Delta E_{\mathrm{XC}}^{\mathrm{LM}} \quad (37)$$

V. Computational Details

To test our approach to approximate IP, EA, and HM, eqs 21, 24, and 33 were programmed in a development version of the NWChem V4.5 code.[29] Integrals are evaluated at the end of the self-consistent cycle, and results are obtained in a single program execution. The exchange-correlation functionals used are Dirac (Slater)[30] and SVWN[30,31] for LDA, Becke[32] and BLYP[32,33] for GGA, and B3LYP for the hybrid method.[34] The results obtained with these exchange-correlation functionals are compared with the orbitals energies obtained with exchange potentials that exhibit correct asymptotic behavior such as HF and the exact local multiplicative exchange potential (v_x^{exact}). Details about the v_x^{exact} can be found in ref 15. The most important characteristic of this potential is that it gives KS orbitals that reproduce HF densities. Additionally, the vertical energy differences (ΔE_{V}) of each process were evaluated according to the ΔSCF method, where on the neutral system geometry the energy is computed when the number of electrons or spin is changed. Thus results from eqs 21, 24, and 33 will be compared with vertical energy changes.

The systems used to test the reliability of this approach are LiH, FH, H_2O, NH_3, and CH_4, and experimental geometries for these systems were used. Since the virtual orbital energies are involved in our approach, we used the aug-cc-pVTZ[35] with an additional diffuse function as a basis set. We used this basis set because the diffuse functions have a big impact in the description of DFT and HF virtual orbitals and in the anions.[14b,20d] As it was mentioned in section II, the most important feature of the approach presented in this work is that we are just using information from the ground state. The additional effort after the self-consistent process corresponds to the evaluation of the integrals $J[\Delta\rho_\alpha + \Delta\rho_\beta]$, $E_{\mathrm{XC}}[\rho_\alpha + \Delta\rho_\alpha, \rho_\beta + \Delta\rho_\beta]$, $\int \mathrm{d}\mathbf{r}\Delta\rho_\alpha(\mathbf{r})v_{\mathrm{XC},\alpha}(\mathbf{r})$, and $\int \mathrm{d}\mathbf{r}\Delta\rho_\beta(\mathbf{r})v_{\mathrm{XC},\beta}(\mathbf{r})$. It means that after the self-consistent process J and E_{XC} must be evaluated with the difference $\Delta\rho_\alpha$ and $\Delta\rho_\beta$, such differences depend on the process to be considered and they are frontier orbital densities. Additionally, the exchange-correlation potential for each spin-component is integrated with its respective density difference.

VI. Results and Discussion

Ionization Potential. Three approximations for the ionization potential reported in Table 1 are (1) the negative of the HOMO eigenvalue obtained with the exchange-correlation functionals considered in this work, (2) the frozen core approximation given by eq 21 and, (3) the direct computation of the vertical energy difference (ΔE_{V}), the cation minus the neutral system. The behavior of these quantities is depicted in Figure 1. All of these estimations for the ionization potential are compared in Table 1 with the experimental information[36] and with the HOMO energy obtained with exchange potentials that exhibit good asymptotic behavior, such as the HF potential and the local multiplicative exchange potential, v_x^{exact}.

From Table 1 and Figure 1, it is evident the well-known fact that the HOMO energy obtained from the usual DFT exchange-correlation potentials underestimates the ionization potential. This observation led to assume that the HOMO from KS theory was not directly related with the ionization potential since LDA, GGA and hybrid methods are not satisfying the relation $\mathrm{IP} = -\epsilon_{\mathrm{HOMO}}$. Contrary to this behavior, exchange potentials with the correct asymptotic behavior give HOMO energies close to the experimental ionization potential, although they slightly overestimate this quantity.

According to eq 21, the additional terms of the HOMO energy are related to the contribution of the non-canceled self-interaction by the usual exchange-correlation functionals. Note

TABLE 1: Estimations for the Ionization Potential in Hartrees

method		system				
		LiH	FH	H_2O	NH_3	CH_4
Slater	$-\epsilon_{HOMO}$	0.1284	0.3109	0.2254	0.1880	0.3018
	eq 21	0.2898	0.6808	0.5319	0.4426	0.5093
	ΔE_V	0.2443	0.5561	0.4277	0.3604	0.4690
Becke	$-\epsilon_{HOMO}$	0.1389	0.3213	0.2346	0.1977	0.3165
	eq 21	0.3099	0.6841	0.5361	0.4486	0.5212
	ΔE_V	0.2631	0.5574	0.4295	0.3646	0.4821
SVWN	$-\epsilon_{HOMO}$	0.1613	0.361	0.2719	0.2322	0.3482
	eq 21	0.3422	0.7392	0.5872	0.4965	0.5619
	ΔE_V	0.3016	0.6162	0.4843	0.4154	0.5232
BLYP	$-\epsilon_{HOMO}$	0.1588	0.3543	0.265	0.226	0.3449
	eq 21	0.3433	0.7243	0.5742	0.4857	0.5663
	ΔE_V	0.3003	0.5993	0.4692	0.4033	0.5166
B3LYP	$-\epsilon_{HOMO}$	0.1953	0.4245	0.3246	0.2774	0.396
	eq 21	0.3465	0.7237	0.575	0.4878	0.5629
	ΔE_V	0.3044	0.5999	0.4705	0.4060	0.5246
HF	$-\epsilon_{HOMO}$	0.3015	0.6503	0.5103	0.4316	0.5455
ν_x^{exact}	$-\epsilon_{HOMO}$	0.3031	0.6421	0.5054	0.4308	0.5349
exp IP		0.28[a]	0.59[a]	0.46[b]	0.38[b]	0.48[b]

[a] Ref 36a. [b] Ref 36b

that the values from Table 1 show that the hybrid B3LYP functional presents the smallest spurious contribution on each molecule.

Comparing the vertical energy difference for all functionals with the experimental ionization potential, we see that the inclusion of a correlation functional, such as VWN or LYP, is important in order to obtain better approximations to the experimental data. One can observe that vertical energies overestimate the IP. The reason of this behavior comes from the lack of the relaxation in the geometry. Remember that in this work we have used experimental geometries to test our approach. Let us work with one molecule with one of the largest differences with respect to the experiment; NH_3 with 0.023 and 0.026 hartrees for BLYP and B3LYP, respectively. If we optimize the neutral system with the BLYP method and the IP is estimated with the ΔSCF method, it is found an IP of 0.4006 hartrees. If the geometry of the cation is optimized, the predicted adiabatic IP is 0.3734 hartrees, which give a better comparison with respect to the experimental information. That means that for the NH_3 molecule the geometry relaxation contribute in 0.0272 hartrees. It is important to point out that we picked the BLYP and B3LYP functionals to make this comparison since they give a good prediction of the IP when the adiabatic process is considered.

As we mentioned before, our frozen core approach is based in the absence of relaxation in the geometry and the orbitals. For this reason the results obtained from eq 21 must be compared with the vertical energy differences, and the difference obtained between both cases must be attributed to the lack of relaxation of the orbitals. In Table 2, the absolute error between eq 21 and the vertical ionization potential is reported. From this table it is clear that the lack of relaxation of the orbitals in eq 21 is important. For all molecules and all exchange-correlation functionals considered in this work, eq 21 overestimates the vertical ionization potential due to the absence of relaxation in the orbitals, this trend is in agreement with eq 20. It is interesting to note that the overestimation obtained for a given molecule with any exchange-correlation functional is almost constant. This fact seems to indicate that the relaxation

TABLE 2: Error between the IP Estimated by Equation 21 and the Vertical Energy Difference

method	system				
	LiH	FH	H_2O	NH_3	CH_4
Slater	0.0455	0.1247	0.1042	0.0822	0.0403
Becke	0.0468	0.1267	0.1066	0.0840	0.0391
SVWN	0.0406	0.1230	0.1029	0.0811	0.0387
BLYP	0.0430	0.1250	0.1050	0.0824	0.0497
B3LYP	0.0421	0.1238	0.1045	0.0818	0.0383
average	0.0436	0.1246	0.1046	0.0823	0.0412

of the orbitals in DFT for the vertical IP is not very sensitive to the type of the exchange-correlation functional used, even if a correlation functional is not considered. The average of the overestimation in the IP obtained with eq 21 for each molecule also is reported in Table 2. The largest overestimation corresponds to the molecule FH with an average of 0.1246 hartrees. Although we are obtaining an overestimation of the IP using eq 21, this prediction is much better than that coming from the HOMO energy obtained with the same exchange-correlation functionals, as it can be seen from Table 1.

Using the BLYP method as reference for the vertical IP, we can compare these values with the HOMO energies obtained with HF and ν_x^{exact}. We use the BLYP functional as reference since it presents a good performance in the prediction of adiabatic IP and EA.[37] In Figure 2, the vertical ΔE obtained with the BLYP functional is compared with the negative of the HOMO energy obtained with HF and with ν_x^{exact}. From Table 1 and Figure 2 we see that these HOMO energies are closer to the vertical IP than to the adiabatic experimental counterpart. Recently some results showed that the HOMO energies can be improved with the design of exchange-correlation potentials with the correct asymptotic behavior[18b,38] or using a scaling approach.[39]

Electron Affinity. The prediction of electron affinities is a challenge for any quantum chemistry method because the EA is a small quantity compared with the ionization potential. Recently it was shown that DFT gives a good prediction of the adiabatic electron affinity in well-characterized systems.[40] From eq 24 we see that the LUMO energy is related with the electron affinity, in fact within HF theory, in the Koopmans' context, the negative of this orbital energy is directly related with the electron affinity. Like in the ionization process, the additional terms in eq 24 are related with the self-interaction energy.

In Table 3, the vertical electron affinities (ΔE_V) for the molecules considered in this work are presented. These vertical electron affinities are compared with the negative of the LUMO energy obtained with all exchange-correlation functionals tested. From this table, ΔE_V shows that only the LiH molecule has an anion that is more stable than the corresponding neutral molecule. This means that the EA estimated by ΔE_V is negative in all the other studied molecules. Contrary to this behavior, with all the exchange-correlation potentials tested here, the estimation to the electron affinity given by the LUMO energy is always positive. The sign of this orbital energy, shown in Table 3, is different to that obtained with ΔE_V. The main point here is that the LUMO energies obtained with any of the used exchange-correlation functionals give a bad approximation to the EA, since all of them are negative and consequently they yield positive electron affinities. In general the LUMO energy is bound when it is obtained with the usual exchange-correlation potentials, although its value is small. In ref 22b the difference between HF and KS potentials is addressed. The frozen core estimation given by eq 24 is also presented in Table 3, and trends are shown in Figure 3. It can also be seen from Table 3

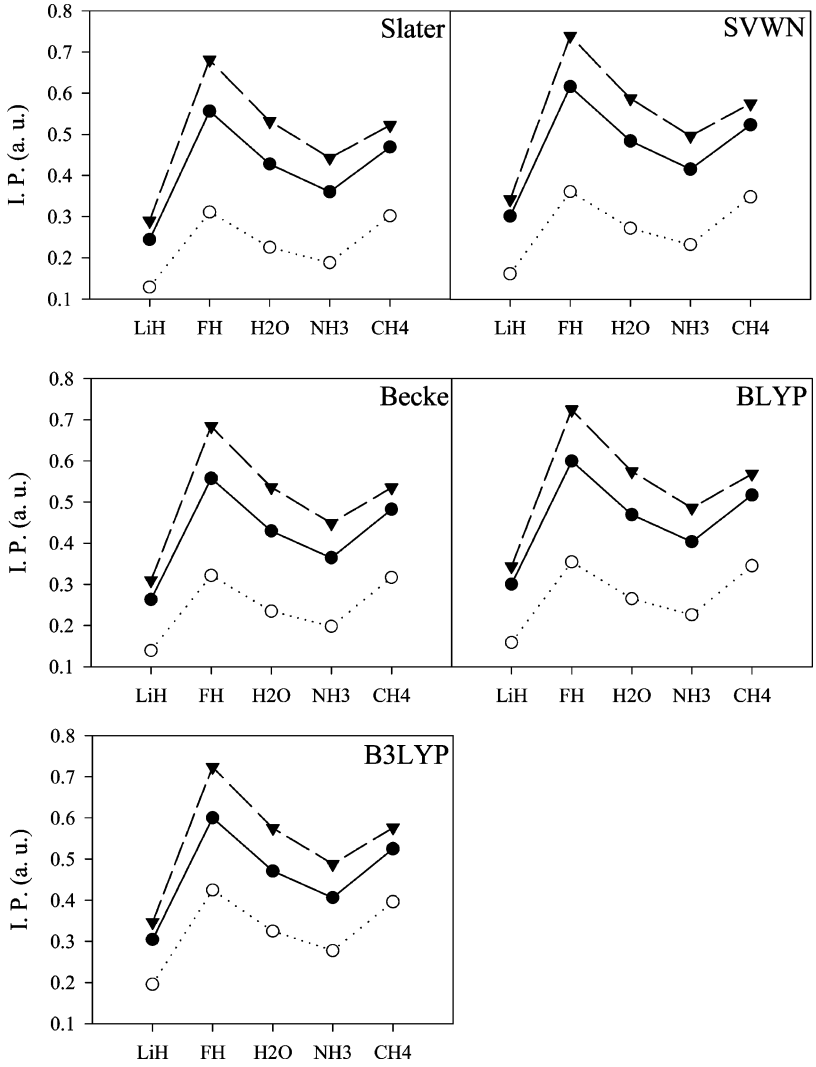

Figure 1. Ionization potential. The solid circles indicate the vertical ionization potential, the open circles indicate the negative of the HOMO energies, and the triangles indicate the estimation obtained from eq 21.

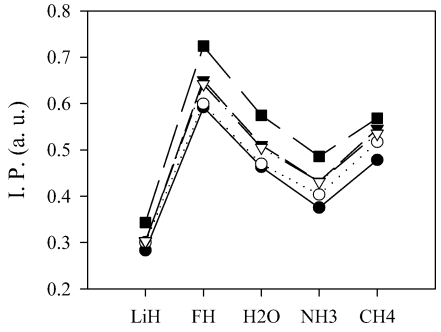

Figure 2. Ionization potential. The solid circles correspond to the experimental values, the open circles correspond to the BLYP vertical values, the solid triangles correspond to the negative of the HF HOMO, the open triangles correspond to the negative of the HOMO obtained with the v_x^{exact} potential, and the solid squares correspond to the BLYP frozen core approximation.

that if exchange-correlation potentials with the correct asymptotic potential are used, LUMO energies are bound and more negative. This behavior is not shared by the HF LUMO energy; Table 3 shows that its value is positive, except for LiH, and very close to zero. In Figure 4, the behavior of the negative LUMO energies obtained with HF and with the local multiplicative potential v_x^{exact} is presented. Both energies are compared with the vertical EA obtained with the BLYP functional. From this figure it is clear that the trend exhibited by the LUMO obtained with the v_x^{exact} potential is very different to that obtained with HF, which is a different behavior with respect to

TABLE 3: Estimations for the Electron Affinity in Hartrees

method		system				
		LiH	FH	H_2O	NH_3	CH_4
Slater	$-\epsilon_{\text{LUMO}}$	0.0412	0.0155	0.0159	0.0110	0.0023
	eq 24	−0.0156	−0.0393	−0.0350	−0.0295	−0.0226
	ΔE_{V}	0.0057	−0.0111	−0.0105	−0.0103	−0.0109
Becke	$-\epsilon_{\text{LUMO}}$	0.0487	0.0260	0.0256	0.0199	0.0103
	eq 24	−0.0060	−0.0365	−0.0314	−0.0271	−0.0237
	ΔE_{V}	0.0120	−0.0064	−0.0062	−0.0063	−0.0066
SVWN	$-\epsilon_{\text{LUMO}}$	0.0561	0.0344	0.0343	0.0268	0.0136
	eq 24	−0.0033	−0.0414	−0.0330	−0.0281	−0.0237
	ΔE_{V}	0.0163	−0.0010	−0.0007	−0.0014	−0.0032
BLYP	$-\epsilon_{\text{LUMO}}$	0.0621	0.0413	0.0396	0.0316	0.0190
	eq 24	−0.0081	−0.0428	−0.0345	−0.0304	−0.0277
	ΔE_{V}	0.0145	−0.0041	−0.0039	−0.0047	−0.0062
B3LYP	$-\epsilon_{\text{LUMO}}$	0.0511	0.0267	0.0262	0.0205	0.0107
	eq 24	0.0010	−0.0266	−0.0225	−0.0201	−0.0182
	ΔE_{V}	0.0165	−0.0016	−0.0016	−0.0023	−0.0038
HF	$-\epsilon_{\text{LUMO}}$	0.0078	−0.0078	−0.0083	−0.0081	−0.0086
v_x^{exact}	$-\epsilon_{\text{LUMO}}$	0.1619	0.2212	0.1976	0.1706	0.1515

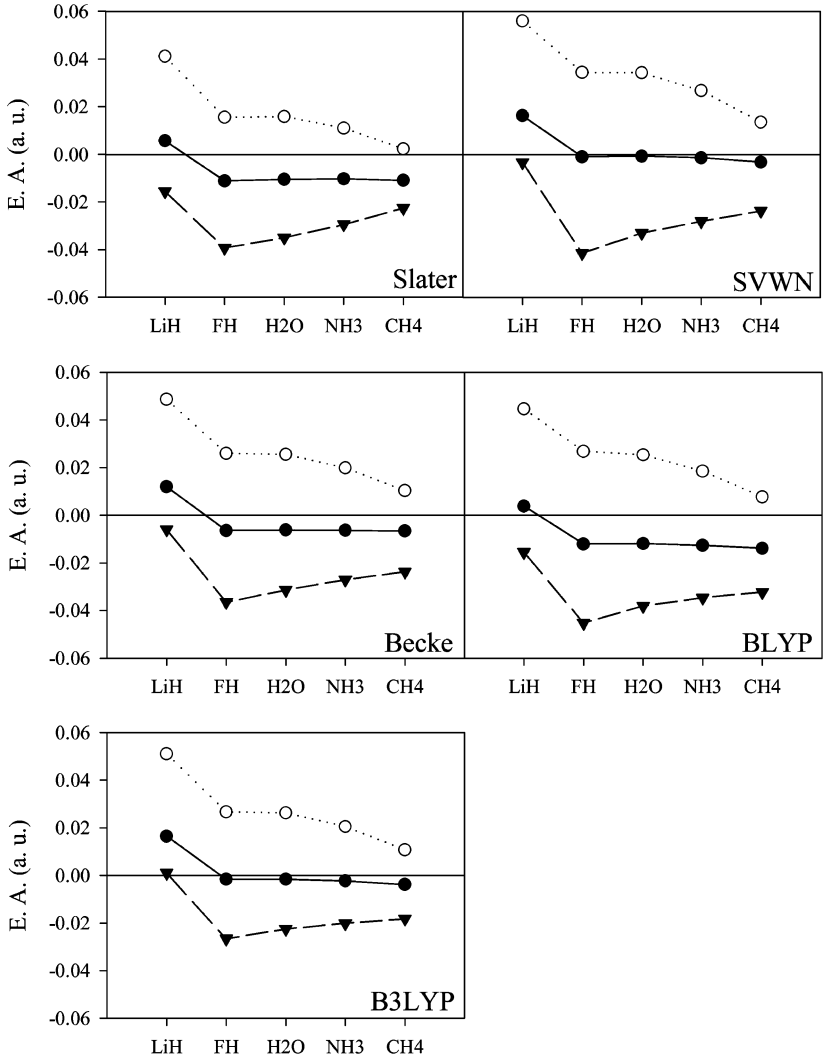

Figure 3. Electron affinity. The solid circles indicate the vertical electron affinity, the open circles indicate the negative of the LUMO energies, and the triangles indicate the estimation obtained from eq 24.

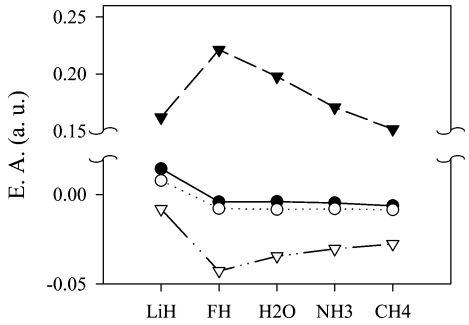

Figure 4. Electron affinity. The solid circles indicate the BLYP vertical values, the open circles indicate the negative of the HF LUMO energies, the solid triangles indicate the negative of the LUMO obtained with the v_x^{exact} potential, and the blank triangles indicate the BLYP frozen core approximation.

the ionization potential where both methods give essentially the same trend. The main reason of such a difference stems in that HF and local-multiplicative potentials exhibit a different behavior for the virtual orbitals, as it has been discussed in previous work.[22b] Note that the use of additional diffuse functions, for example in the aug-cc-pVTZ basis set, generates an improvement to the HF LUMO energies and the trend exhibited by these energies is similar to that obtained with the vertical EA.

The frozen core approximation gives a better estimation of EA, however the corresponding values underestimate this energy difference (eq 20) and EA values obtained from eq 24 are negative in all cases, except for the B3LYP functional where the sign is correctly predicted. Since the present approach approximates the energy of the anion with the orbitals from the neutral species, it is assumed that the new orbital remains unchanged. The results show that this assumption does not hold. In the process of adding one electron to a molecule, the KS orbital relaxation plays a very important role, which may lead to important errors.

In summary, the ionization potential can be reasonably approximated from eq 21 or directly using the HOMO energy obtained from v_x^{exact} potential. The trend exhibited by the HOMO energy obtained with the exchange-correlation potentials considered in this work is similar to those obtained with the vertical ionization potentials. Contrary to this behavior the sign of the vertical electron affinity cannot be reproduced by the LUMO energy obtained with any exchange-correlation potential, neither with the local multiplicative potential, v_x^{exact}. Thus, the negative of the LUMO energy obtained from an exchange-correlation potential with the correct asymptotic behavior must not be used as an approximation to the EA. Consequently the anomalies presented by the LUMO energies will affect the description of the χ, η, and ω obtained from these quantities.

TABLE 4: Electronegativity Obtained with the HOMO and LUMO Energies, the Frozen Core Approximation, and the Vertical Energy Differences[a]

		system				
	method	LiH	FH	H_2O	NH_3	CH_4
Slater	orbital energies	0.0848	0.1632	0.1207	0.0995	0.1521
	frozen core	0.1371	0.3208	0.2485	0.2066	0.2434
	vert. difference	0.1250	0.2725	0.2086	0.1751	0.2291
Becke	orbital energies	0.0938	0.1737	0.1301	0.1088	0.1634
	frozen core	0.1520	0.3238	0.2524	0.2108	0.2488
	vert. difference	0.1375	0.2755	0.2116	0.1791	0.2377
SVWN	orbital energies	0.1087	0.1977	0.1531	0.1295	0.1809
	frozen core	0.1695	0.3489	0.2771	0.2342	0.2691
	vert. difference	0.1589	0.3076	0.2418	0.2070	0.2600
BLYP	orbital energies	0.1105	0.1978	0.1523	0.1288	0.1820
	frozen core	0.1676	0.3408	0.2699	0.2277	0.2693
	vert. difference	0.1574	0.2976	0.2326	0.1993	0.2552
B3LYP	orbital energies	0.1232	0.2256	0.1754	0.1490	0.2034
	frozen core	0.1738	0.3486	0.2763	0.2339	0.2724
	vert. difference	0.1604	0.2992	0.2344	0.2018	0.2604
HF	orbital energies	0.1547	0.3213	0.2510	0.2118	0.2685
ν_x^{exact}	orbital energies	0.2325	0.4317	0.3515	0.3007	0.3432

[a] Values reported in hartrees.

This problem does not apply to the HF orbital energies since these energies give reasonable approximations to IP and EA.

Electronegativity. This quantity was obtained by using the vertical IP and EA according to the finite difference approximation $\chi = {}^1/_2(\text{IP} + \text{EA})$. Estimation of IP and EA is done with the following approximations: (1) vertical energies, ΔE_V; (2) frozen core, eq 28; (3) HOMO and LUMO energies. These results are reported in Table 4.

Since the electron affinity is a small quantity, in general the electronegativity behavior is commanded by the ionization potential. Although the LUMO energies obtained with any of the tested exchange-correlation functionals are negative, they are close to zero. Consequently the electronegativity trend from HOMO and LUMO energies, obtained with these functionals, is similar to that obtained with the HOMO energy for the estimation of IP (see Figure 1).

It is evident that, in absolute values, the estimation of χ with the KS orbital energies is not good. However, the underestimation of χ given by the orbital energies is modified in the correct direction by the frozen core approximation proposed in this work; moreover, this approach presents a small overestimation of such quantity. Thus, the prediction made by the frozen core approximation is better than that obtained by the HOMO and LUMO energies.

In Figure 5, the electronegativity from the vertical energy differences obtained with the BLYP functional is compared with the χ estimated with the orbital energies from HF and ν_x^{exact} potentials. Without doubt the trend obtained for this quantity with the HF orbital energies is very similar to that obtained with the vertical BLYP energy differences; in fact the absolute values between these two methods are in good agreement. In opposition to the previous methods, the electronegativity estimated with the orbital energies from ν_x^{exact} is greater than that obtained with the vertical energy difference, since the LUMO energy obtained from ν_x^{exact} is very deep.

Hardness. As it was mentioned above, the hardness is estimated as $\eta = (\text{IP} - \text{EA})$. Here we again used the same approximations for the IP and EA: (1) vertical energies; (2) frozen core, eq 29; (3) HOMO and LUMO energies. The results are reported in Table 5.

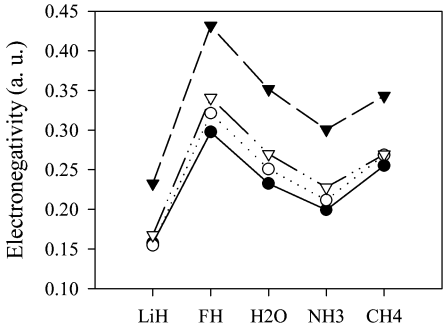

Figure 5. Electronegativity estimated with the BLYP vertical energy differences (solid circles), HF orbital energies (open circles), ν_x^{exact} orbital energies (solid triangles), and BLYP frozen core approximation (open triangles).

TABLE 5: Hardness Obtained with the HOMO and LUMO Energies, the Frozen Core Approximation, and the Vertical Energy Differences[a]

		system				
	method	LiH	FH	H_2O	NH_3	CH_4
Slater	orbital energies	0.0872	0.2954	0.2095	0.1770	0.2995
	frozen core	0.3054	0.7201	0.5669	0.4721	0.5319
	vert. difference	0.2386	0.5673	0.4382	0.3707	0.4799
Becke	orbital energies	0.0902	0.2953	0.2090	0.1778	0.3062
	frozen core	0.3159	0.7206	0.5675	0.4757	0.5449
	vert. difference	0.2512	0.5638	0.4357	0.3709	0.4887
SVWN	orbital energies	0.1052	0.3266	0.2376	0.2054	0.3346
	frozen core	0.3455	0.7806	0.6202	0.5246	0.5856
	vert. difference	0.2853	0.6172	0.4849	0.4167	0.5264
BLYP	orbital energies	0.0967	0.3130	0.2254	0.1944	0.3259
	frozen core	0.3514	0.7671	0.6087	0.5161	0.5940
	vert. difference	0.2858	0.6035	0.4731	0.4080	0.5227
B3LYP	orbital energies	0.1442	0.3978	0.2984	0.2569	0.3853
	frozen core	0.3455	0.7503	0.5975	0.5079	0.5811
	vert. difference	0.2879	0.6015	0.4721	0.4083	0.5285
HF	orbital energies	0.2937	0.6581	0.5186	0.4397	0.5541
ν_x^{exact}	orbital energies	0.1412	0.4209	0.3079	0.2602	0.3834

[a] Values reported in hartrees.

The hardness obtained with the eq 29 and with the HOMO and LUMO energies show a similar trend to that obtained with the vertical energy differences. Comparing results from Table 1 and Table 5, it is clear that the behavior exhibited by the hardness is similar to that of the ionization potential with any of the exchange-correlation potentials used in this work, since the LUMO energies are very small. Although the electron affinity is underestimated by the frozen core approach, the trend is similar to that from the vertical energy differences. In Table 5 the hardness obtained with the three approaches to IP and EA is reported. From this table we can see that the frozen core approach gives a better estimation of the hardness than that obtained just with the KS HOMO and LUMO energies. Overestimation of the hardness by the frozen core approach shown in Table 5 is a consequence of eq 20.

In Figure 6, the hardness obtained with the BLYP vertical energy differences and with HOMO and LUMO energies from the HF and ν_x^{exact} potentials is depicted. It is clear that the HF frontier orbital energies give a reasonable estimation of hardness. Contrary to this behavior, the hardness values calculated with the frontier orbital energies from the local multiplicative potential (ν_x^{exact}) underestimate the BLYP vertical energy dif-

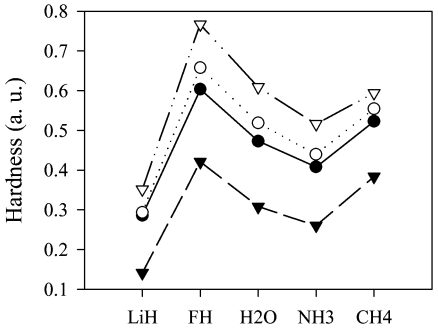

Figure 6. Hardness estimated with the BLYP vertical energy differences (solid circles), with HF orbital energies (open circles), ν_x^{exact} orbital energies (solid triangles), and BLYP frozen core approximation (open triangles).

TABLE 6: Electrophilicity Obtained with the HOMO and LUMO Energies, the Frozen Core Approximation, and the Vertical Energy Differences[a]

method		system				
		LiH	FH	H_2O	NH_3	CH_4
Slater	orbital energies	0.0412	0.0451	0.0347	0.0280	0.0386
	frozen core	0.0308	0.0714	0.0544	0.0452	0.0557
	vert. difference	0.0327	0.0654	0.0497	0.0414	0.0547
Becke	orbital energies	0.0488	0.0511	0.0405	0.0333	0.0436
	frozen core	0.0365	0.0727	0.0561	0.0467	0.0568
	vert. difference	0.0377	0.0673	0.0514	0.0432	0.0578
SVWN	orbital energies	0.0562	0.0598	0.0493	0.0408	0.0489
	frozen core	0.0416	0.0780	0.0619	0.0523	0.0618
	vert. difference	0.0443	0.0766	0.0603	0.0514	0.0642
BLYP	orbital energies	0.0631	0.0625	0.0515	0.0427	0.0508
	frozen core	0.0400	0.0757	0.0598	0.0502	0.0610
	vert. difference	0.0433	0.0734	0.0572	0.0487	0.0623
B3LYP	orbital energies	0.0526	0.0640	0.0516	0.0432	0.0537
	frozen core	0.0437	0.0810	0.0639	0.0538	0.0638
	vert. difference	0.0447	0.0744	0.0582	0.0499	0.0642
HF	orbital energies	0.0407	0.0784	0.0607	0.0510	0.0650
ν_x^{exact}	orbital energies	0.1914	0.2213	0.2006	0.1738	0.1536

[a] Values reported in hartrees.

ferences, roughly in one-half. Curiously, the hardness values from the frontier orbitals of B3LYP and the local multiplicative potential are very similar. Thus, we can conclude that the orbital energies obtained with a local multiplicative potential such, as LDA, GGA or ν_x^{exact} must not be used to estimate the hardness of a chemical system. This observation can be applied to any KS local multiplicative potential.

Electrophilicity. In Table 6 the electrophilicity computed from χ and η with the three previously discussed approaches is reported. From the previous analysis of the KS orbital energies performance, it is clear that the use of the HOMO and LUMO KS energies is not suitable for the estimation of this property. In fact, if orbital energies from an exchange-correlation potential with the correct asymptotic behavior are used, the estimation of ω becomes worst, with respect to those values obtained with vertical differences to IP and EA. Contrary to this behavior the HF orbital energies give a good estimation of ω. It is worth to note that the frozen core approximation proposed in this work gives values of ω close to those obtained with the vertical energy differences. These trends are shown in Figure 7.

From previous sections we can conclude that for the estimation of χ, η, and ω with orbital energies it is only recommendable to use the HF approach, but if the KS approach is used, then the frozen core approach proposed in this work must be used in order to get a better approximation.

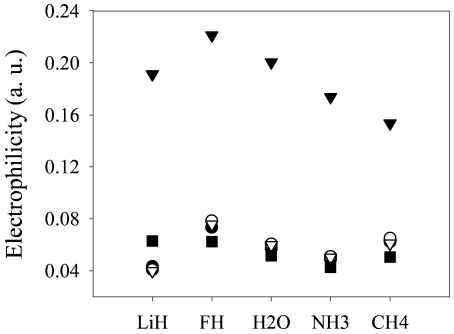

Figure 7. Electrophilicity estimated with the BLYP vertical energy differences (solid circles), HF orbital energies (open circles), ν_x^{exact} orbital energies (solid triangles), BLYP frozen core approximation (open triangles), and BLYP orbital energies (solid squares).

TABLE 7: Estimations for Vertical Excitation Energies Singlet−Triplet[a]

method		system				
		LiH	FH	H_2O	NH_3	CH_4
Slater	$\epsilon_L - \epsilon_H$	0.0872	0.2955	0.2095	0.1770	0.2994
	eq 33	0.1194	0.4809	0.3460	0.2891	0.3999
	ΔE_V	0.0812	0.3487	0.2396	0.2017	0.3575
Becke	$\epsilon_L - \epsilon_H$	0.0902	0.2953	0.2090	0.1778	0.3062
	eq 33	0.1304	0.4724	0.3426	0.2879	0.4014
	ΔE_V	0.0893	0.3394	0.2331	0.1995	0.3630
SVWN	$\epsilon_L - \epsilon_H$	0.1053	0.3267	0.2376	0.2053	0.3346
	eq 33	0.1548	0.4954	0.3620	0.3085	0.4175
	ΔE_V	0.1222	0.3839	0.2721	0.2353	0.3874
BLYP	$\epsilon_L - \epsilon_H$	0.0967	0.3130	0.2254	0.1944	0.3259
	eq 33	0.1576	0.4866	0.3571	0.3052	0.4162
	ΔE_V	0.1221	0.3686	0.2601	0.2271	0.3853
B3LYP	$\epsilon_L - \epsilon_H$	0.1442	0.3978	0.2983	0.2569	0.3853
	eq 33	0.1616	0.5021	0.3705	0.3161	0.4321
	ΔE_V	0.1221	0.3663	0.2598	0.2284	0.3927
HF	$\epsilon_L - \epsilon_H$	0.2937	0.6581	0.5186	0.4397	0.5541
ν_x^{exact}	$\epsilon_L - \epsilon_H$	0.1412	0.4209	0.3079	0.2602	0.3834
experiment		0.12[b]	0.38[b]	0.26[c]	0.21[d]	0.40[c]

[a] Values reported in hartrees. [b] Ref 36a. [c] Ref 41. [d] Ref 36b.

Excitation Energies. Up to now, quantities related with energy differences due to changes in the number of electrons have been discussed. Here energy differences due to multiplicity changes, where the number of electrons remains fixed, are discussed. In particular, we are interested in changes where a closed-shell system transforms into a vertical triplet state (vertical singlet−triplet splitting), and this process corresponds to a vertical excitation energy. In Table 7 several approximations to vertical excitation energies, for all exchange-correlation functionals tested, are reported: (1) the vertical triplet−singlet energy difference, (2) frozen core (eq 33), and (3) orbital energy difference $\epsilon_{\text{LUMO}} - \epsilon_{\text{HOMO}}$. Experimental vertical excitation energies are also listed.[41]

From Table 7 we note that the vertical excitation energies predicted by DFT are in good agreement with the experimental counterpart. To obtain this agreement it is important to include the correlation energy contribution. Table 8 presents the relative percent error obtained with all exchange-correlation functionals used in this work with respect to the experimental values. From this table, the underestimation of the vertical excitation energies obtained with exchange-only functionals is evident. The inclu-

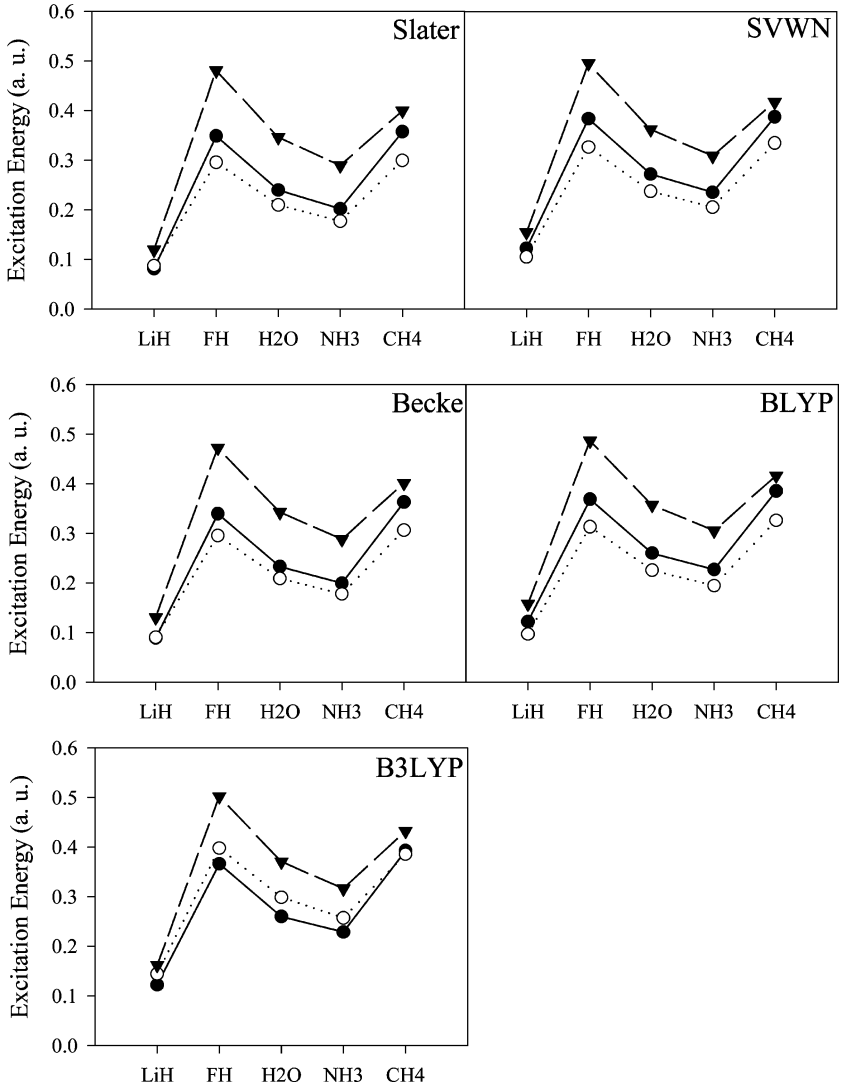

Figure 8. Vertical excitation energies. Solid circles represent vertical energy differences, open circles indicate the orbital energies, and the triangles indicate the estimation obtained from the frozen core approximation, eq 33.

TABLE 8: Relative Percent Error between the Vertical Excitation Energies and Experimental Data

	system				
E_{XC}	LiH	FH	H_2O	NH_3	CH_4
Slater	−32	−8	−8	−4	−11
Becke	−26	−11	−10	−5	−9
SVWN	2	1	5	12	3
BLYP	2	−3	0	8	−4
B3LYP	2	4	0	9	−2

sion of a correlation functional greatly improves the prediction of these quantities, even with the local SVWN functional we can obtain a reasonable approximation, except for the NH_3 where the error increases.

The behavior of the vertical excitation energy for each exchange-correlation functional is depicted in Figure 8. Comparing the excitation energies with the hardness, both obtained with the vertical energy differences, it is clear that they are different. Whereas the difference $\epsilon_{LUMO} - \epsilon_{HOMO}$ gives an evident underestimation of the hardness, this difference is very close to the vertical excitation energies for any exchange-correlation functional of this work.[20,42] Overestimation of the frozen core vertical excitation energies, observed in Table 7, comes from eq 20. Contrary to the results obtained in previous sections, the values from the orbital energy difference are better

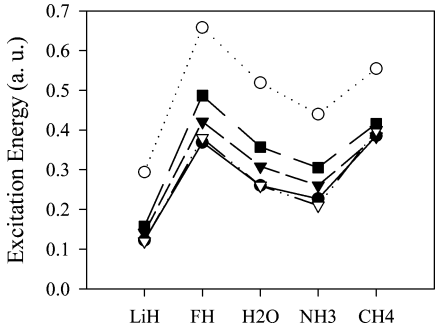

Figure 9. Excitation energies estimated with the BLYP vertical energy differences (solid circles), HF orbital energies (open circles), ν_x^{exact} orbital energies (solid triangles), experimental values (open triangles), and BLYP frozen core approximation (solid squares).

than those obtained from the frozen core approximation. In Figure 9, trends for BLYP vertical excitation energies, HF, and ν_x^{exact} frontier orbital energy differences are compared with experimental data. In opposition to the KS case, the HF orbital energies are not appropriate to approximate excitation energies, an overestimation to this quantity is found, while ν_x^{exact} values slightly overestimate the BLYP vertical values. It is important to note that HF frontier orbital energies are related to removal

or addition of electrons by Koopmans' theorem, but excitation energy does not naturally appear in this model.

VII. Concluding Remarks

In this paper the frontier KS orbitals are used to estimate properties such as electronegativity, hardness, electrophilicity, and excitation energies in the frozen core approximation. It is clear from the present approach that these quantities are not only related with HOMO and LUMO energies, but also additional contributions appear. These contributions can be associated with the incomplete cancellation of the self-interaction, which is present in many of the currently used exchange-correlation functionals.

Our results show that for the ionization process, the additional contribution is larger for the local (SVWN) exchange-correlation functional, while the smallest corresponds to the hybrid B3LYP functional. Furthermore, the trend for the KS HOMO and the vertical ionization potentials is the same. On the other hand, the sign of the LUMO energy does not match that of the vertical electron affinities. In consequence the description of η, χ, and ω is affected when only HOMO and LUMO energies are used. In this way, the frozen core approximation presented here provides a better way to estimate these reactivity descriptors. It is very evident that electrophilicity index values obtained from KS frontier orbital energies do not follow the trend shown by the vertical energies, which is similar to the frozen core values. Contrary to this behavior, the HF orbital energies show a good comparison with the ionization potential and electron affinity. Consequently, the reactivity descriptors considered in this work are well-described with this method. For the excitation energies, KS frontier orbital differences give better results than the frozen core approach, and the estimations from the HF orbital energies are largely overestimated. It is important to mention that the Hartree−Fock LUMO energy gives a good correlation with the electron affinity, which is not true for the LUMO energy obtained with any exchange-correlation potential. Thus the physical meaning for the LUMO energy is quite different between Hartree−Fock and Kohn−Sham approaches.

In general, the frozen core approach presented here enhances the estimations obtained with KS orbital energies, with one exception. For excitation energies, the KS energy differences provide better results than the frozen core approximation. Thus, the better numerical values come from the following strategy: Use a correlated method, such a BLYP or B3LYP, to optimize the molecular geometry; on that geometry compute the electronic structure with the HF method; use the HF orbital energies to estimate η, χ, and ω. For the singlet−triplet splitting, the KS orbital energies give a reasonable approximation. Inclusion of spin-polarized chemical indexes can be done if appropriate restrictions are applied.[6,26,43]

Acknowledgment. Financial support from CONACYT-México was provided by project 39622-F. We thank to the Laboratorio de Visualización y Supercómputo en Paralelo at UAM-Iztapalapa for the access to its computer facilities.

References and Notes

(1) Parr, R. G.; Yang, W. *Density Functional Theory of Atoms and Molecules*; Oxford University Press: New York, 1989.

(2) Koch, W.; Holthaussen, M. C. *A Chemist's Guide to Density Functional Theory*; Wiley-VCH: Weinheim, 2000.

(3) Parr, R. G.; Donelly, D. A.; Levy, M.; Palke, W. E. *J. Chem. Phys.* **1978**, *68*, 3801.

(4) Parr, R. G.; Pearson, R. G. *J. Am. Chem. Soc.* **1983**, *105*, 7512.

(5) Yang, W.; Parr, R. G. *Proc. Natl. Acad. Sci. U.S.A.* **1985**, *82*, 6723.

(6) Galván, M.; Vela, A.; Gázquez, J. L. *J. Phys. Chem.* **1988**, *92*, 6470.

(7) Parr, R. G.; von Szentpaly, L.; Liu, S. *J. Am. Chem. Soc.* **1999**, *121*, 1922.

(8) (a) Fukui, K. *Science*, **1987**, *218*, 747. (b) Parr, R. G.; Yang, W. *J. Am. Chem. Soc.* **1984**, *106*, 4049.

(9) Hohenberg, P.; Kohn, W. *Phys. Rev.* **1964**, *136*, B864.

(10) Kohn, W.; Sham, L. J. *Phys. Rev. A*, **1965**, *140*, 1133.

(11) Koopmans, T. A. *Physica* **1933**, *1*, 104.

(12) Geerlings, P.; De Proft, F.; Langenaeker, W. *Chem. Rev.* **2003**, *103*, 1793.

(13) Gutierrez-Oliva, S.; Jaque, P.; Toro-Labbé, A. In *Reviews of Modern Quantum Chemistry*; Sen, K. D., Ed.; World Scientific: Singapore, 2002, Vol. 1, p 966.

(14) (a) Baerends, E. J.; Gritsenko, O. V. *J. Phys. Chem. A* **1997**, *101*, 5383. (b) Garza, J.; Fahlstrom, C. A.; Vargas, R.; Nichols, J. A.; Dixon, D. A. In *Reviews of Modern Quantum Chemistry*; Sen, K. D., Ed.; World Scientific: Singapore, 2002; Vol. 2, p 1508. (c) Stowasser, R.; Hoffman, R. *J. Am. Chem.* Soc. **1999**, *121*, 3414.

(15) Garza, J.; Nichols, J. A.; Dixon, D. A. *J. Chem. Phys.* **2000**, *113*, 6029.

(16) (a) Perdew, J. P.; Parr, R. G.; Levy, M.; Balduz Jr., J. L. *Phys. Rev. Lett.* **1982**, *49*, 1691. (b) Perdew, J. P.; Levy, M. *Phys. Rev. B* **1997**, *56*, 16021. (c) Görling, A. *Phys. Rev. A.* **1996**, *54*, 3912. (d) Levy, M. *Phys. Rev. A.* **1995**, *52*, R4313. (e) Kim, Y.-H.; Stadele, M.; Martin, R. M. *Phys. Rev. A.* **1999**, *60*, 3633. (f) Umrigar, C. J.; Savin, A.; Gonze, X. *Electronic Density Functional Theory: Recent Progress and New Directions*; Dobson, et al., Eds.; Plenum: New York, 1998; p 167.

(17) (a) Kleinman, L. *Phys. Rev. B* **1997**, *56*, 12042. (b) Kleinman, L. *Phys. Rev. B* **1997**, *56*, 16029. (c) Politzer, P.; Abu-Awwad, F.; Murray, J. S. *Int. J. Quantum Chem.* **1998**, *69*, 607.

(18) (a) Almbladh, C.-O.; von Barth, U. *Phys. Rev. B* **1985**, *31*, 3231. (b) Tozer, D. J.; Ingamells, V. E.; Handy, N. C. *J. Chem. Phys.* **1996**, *105*, 9200.

(19) (a) Gritsenko, O. V.; Baerends, E. J. *J. Chem. Phys.* **2002**, *117*, 9154. (b) Gritsenko, O. V.; Braïda, B.; Baerends, E. J. *J. Chem. Phys.* **2003**, *119*, 1937. (c) Gritsenko, O. V.; Baerends, E. J. *J. Chem. Phys.* **2004**, *120*, 8364.

(20) (a) Perdew, J. P.; Levy, M. *Phys. Rev. Lett.* **1983**, *51*, 1884. (b) Perdew, J. P. *Density Functional Theory*; Dreizler, R. M., da Providencia, J., Eds.; NATO ASI Series B, Vol. 123; Plenum: New York, 1985; p 265. (c) Savin, A.; Umrigar, C. J.; Gonze, X. *Chem. Phys. Lett.* **1998**, *288*, 391. (d) Garza, J.; Nichols, J. A.; Dixon, D. A. *J. Chem. Phys.* **2000**, *112*, 7880. (e) Garza, J.; Vargas, R.; Nichols, J. A.; Dixon, D. A. *J. Chem. Phys.* **2001**, *114*, 639. (f) Wu, Q.; Ayers, P. W.; Yang, W. T. *J. Chem. Phys.* **2003**, *119*, 2978. (g) Ayers, P. W.; Morrison, R. C.; Parr, R. G. *Mol. Phys.* **2005**, *103*, 2061.

(21) (a) Bauernschmitt, R.; Ahlrichs, R. *Chem. Phys. Lett.* **1996**, *256*, 454. (b) Tozer, D. J.; Handy, N. C. *J. Chem. Phys.* **1998**, *109*, 10180.

(22) (a) Garza, J.; Nichols, J. A.; Dixon, D. A. *J. Chem. Phys.* **2000**, *112*, 1150. (b) Aparicio, F.; Garza, J.; Cedillo, A.; Galván, M.; Vargas, R.; in *Reviews of Modern Quantum Chemistry*; Sen, K. D., Ed.; World Scientific: Singapore, 2002; Vol. 1, p 755. (c) Tozer, D. J.; Handy, N. C. *Phys. Chem. Chem. Phys.* **2000**, *2*, 2117. (d) Tozer, D. J.; Handy, N. C. *Mol. Phys.* **2003**, *101*, 2669.

(23) Perdew, J. P.; Zunger, A. *Phys. Rev. B* **1981**, *23*, 5048.

(24) Gopinathan, M. S. *J. Phys. B: Atom. Mol. Phys.* **1979**, *12*, 521.

(25) (a) For example: Marques, M. A. L.; Gross, E. K. U. *Annu. Rev. Phys. Chem.* **2004**, *55* 427. (b) Filippi, C.; Umrigar, C. J.; Gonze, X. *J. Chem. Phys.* **1997**, *107*, 9994.

(26) Galván, M.; Vargas, R. *J. Phys. Chem.* **1992**, *96*, 1625.

(27) Vargas, R.; Galván, M.; Vela, A. *J. Phys. Chem. A* **1998**, *102*, 3134.

(28) Zevallos, J.; Cedillo, A.; Toro-Labbé, A. Manuscript in process.

(29) Bernholdt, D. E.; Apra, E.; Fruchtl, H. A.; Guest, M. F.; Harrison, R. J.; Kendall, R. A.; Dutteh, R. A.; Long, X.; Nicholas, J. B.; Nichols, J. A.; Taylor, H. L.; Wong, A. T.; Fann, G. I.; Littlefield, R. J.; Nieplocha, J. *Int. J. Quantum Chem. Symp.* **1995**, *29*, 475.

(30) Slater, J. C. *Quantum Theory of Molecules and Solids. Vol. 4: The Self-Consistent Fields for Molecules and Solids*; McGraw-Hill: New York, 1974.

(31) Vosko, S. H.; Wilk, L.; Nusair, M. *Can. J. Phys.* **1980**, *58*, 1200.

(32) Becke, A. D. *Phys. Rev. A.* **1988**, *38*, 3098.

(33) Lee, C.; Yang, W.; Parr, R. G. *Phys. Rev. B* **1988**, *37*, 785.

(34) (a) Becke, A. D. *J. Chem. Phys.* **1993**, *98*, 5648. (b) Becke, A. D. *J. Chem. Phys.* **1993**, *98*, 1372.

(35) (a) Dunning, T. H., Jr. *J. Chem. Phys.* **1970**, *53*, 2823. (b) Dunning, T. H. Jr.; Hay, J. P. In *Methods of Electronic Structure Theory*; Schaefer, H. F., III, Ed.; Plenum Press: New York, 1977; Vol. 3.

(36) (a) Huber, K. P.; Herzberg, G. *Molecular Spectra and Molecular Structure IV. Constants of Diatomic Molecules*; Van Nostrand: Princeton, NJ, 1979. (b) Herzberg, G. *Molecular Spectra and Molecular Structure III. Electronic Spectra and Electronic Structure of Polyatomic Molecules*; Van Nostrand: Princeton, NJ, 1966.

(37) De Proft, F.; Geerlings, P. *J. Chem. Phys.* **1997**, *106*, 3270.
(38) (a) Ingamells, V. E.; Handy, N. C. *Chem. Phys. Lett.* **1996**, *248*, 373. (b) Chong, D. P.; Gritsenko, O. V.; Baerends, E. J. *J. Chem. Phys.* **2002**, *116*, 1760.
(39) Hirata, S.; Zhan, C.-G.; Apra, E.; Windus, T. L.; Dixon, D. A. *J. Phys. Chem. A* **2003**, *107*, 10154.
(40) Rienstra-Kivacofe, J. C.; Tschumper, G. S.; Schaefer, H. F., III. *Chem. Rev.* **2002**, *102*, 231.
(41) Hurley, A. C. *Introduction to the Electronic Theory of Small Molecules*; Academic: London, 1976.
(42) Levy, M.; Nagy, Á. *Phys. Rev. A* **1999**, *59*, 1687.
(43) Chermette, H. *J. Comput. Chem.* **1999**, *20*, 129.